Applied Catalysis B: Environmental 210 (2017) 88–96

Contents lists available at ScienceDirect

Applied Catalysis B: Environmental

journal homepage: www.elsevier.com/locate/apcatb

Photodegradation of sulfonamides by g-C_3N_4 under visible light irradiation: Effectiveness, mechanism and pathways

Yali Song, Jiayu Tian*, Shanshan Gao, Penghui Shao, Jingyao Qi*, Fuyi Cui

State Key Laboratory of Urban Water Resource and Environment, School of Municipal and Environmental Engineering, Harbin Institute of Technology, Harbin 150090, PR China

ARTICLE INFO

Article history:
Received 5 November 2016
Received in revised form 22 January 2017
Accepted 24 March 2017
Available online 25 March 2017

Keywords:
Visible light
Photocatalytic degradation
g-C_3N_4
Sulfonamides

ABSTRACT

For the first time, the photocatalytic degradation of sulfamethoxazole (SMX), sulfisoxazole (SSX), sulfadiazine (SDZ), sulfamerazine (SMZ) by g-C_3N_4 under visible light irradiation was investigated. Results revealed that compared to photolysis, the photocatalytic degradation efficiencies of the four sulfonamides were significantly enhanced with the addition of g-C_3N_4, and more than 90% of photodegradation removal was obtained. The effects of typical water quality parameters, including solution pH, bicarbonate ion and humic acid, on the photodegradation process were discussed. It was found that although the photodegradation of the four sulfonamides exhibited different trends under the variation of the water quality parameters, an excellent photocatalytic removal could always be achieved, illustrating the robustness and effectiveness of the g-C_3N_4 photodegradation process. The ESR measurements showed that both $OH^{\bullet}$ and $^{\bullet}O_2^-$ were produced in the photocatalytic process of g-C_3N_4 under visible light irradiation. And trapping experiments confirmed that $^{\bullet}O_2^-$ and holes played a significant role in the photodegradation of SMX, SDZ and SMZ; but holes and $OH^{\bullet}$ were the main oxidative species for SSX degradation. Finally, according to the oxidation products detected by ultra-high performance liquid chromatography-tandem mass spectrometric (UPLC/MS/MS), the degradation pathways of the four sulfonamides were proposed and compared. It was found that there were some common pathways shared by the different sulfonamides, such as cleavage of S-N bond and hydroxylation of the benzene ring (the main degradation pathways for SSX). More importantly, some specific photodegradation pathways were also identified: (1) the nitration of amino group on the benzene ring occurred for SMX, SDZ and SMZ (the main degradation pathway for SMX, SDZ and SMZ), but not for SSX; (2) the bond cleavage between benzene ring and S occurred only in degradation of SSX; and (3) the carboxylation of the methyl group occurred only in degradation of SMZ.

1. Introduction

Antibiotics have been excessively abused in domestic animals and humans to cure or prevent diseases caused by microorganisms [1,2]. As emerging contaminants, they have attracted growing attention in recent years because of their potential threats to aquatic life and human health [1,3]. Sulfonamides, a large group of broad-spectrum antibiotics, have been extensively used since 1968 [4,5]. Detection of sulfonamides in aquatic environment has been also reported by many researchers [6–8]. Among them, sulfamethoxazole was the most frequently detected, followed by sulfamethazine and sulfadiazine [4].

Due to their polarity and antibacterial nature, poor removal of the sulfonamides was exhibited during conventional biological wastewater treatment [3,9,10]. As a result, sulfamethoxazole has been repeatedly detected with concentrations as high as 24.8 $\mu g\,L^{-1}$ in wastewater treatment plant secondary effluent and 940 $ng\,L^{-1}$ in surface water [11–14]. Previous studies also demonstrated that sulfamethoxazole cannot be effectively eliminated during conventional drinking water treatment processes (coagulation, sedimentation and sand-filtration) [2,14]. Thus, an effective elimination of the sulfonamides from surface water is very important for protecting the human health and ecological safety. For better removal of the sulfonamides, a lot of advanced water treatment methods have been investigated, such as ozonation, activated carbon adsorption, photocatalysis and electrolysis [10,15–17]. Among which, photocatalysis has recently received tremendous research attention because it is green and efficient [16,18].

* Corresponding authors.
E-mail addresses: tjy800112@163.com (J. Tian), jyq@hit.edu.cn (J. Qi).

http://dx.doi.org/10.1016/j.apcatb.2017.03.059
0926-3373/

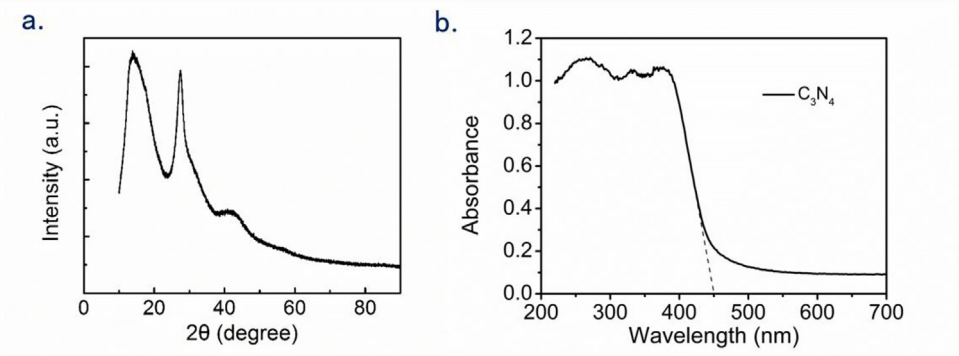

Fig. 1. (a) XRD and (b) UV–vis spectrum of the synthesized g-C_3N_4.

Graphitic carbon nitride (g-C_3N_4), a polymeric metal-free semiconductor, can absorb visible light due to its band gap of 2.70 eV and is stable in solutions with pH 0–14 under the light irradiation [19]. g-C_3N_4 has attracted more and more research interest in the photocatalytic field due to its physicochemical stability, excellent efficiency, easy preparation via cheap materials, and environmental friendliness [20,21]. Yan et al. has reported that methyl orange (MO) could be effectively photodegraded by g-C_3N_4, prepared by heating melamine at different temperature, as demonstrated by as high as 89% of MO (0.4 mg L^{-1}) removal under visible light irradiation [22]. Jing et al. also reported that an effective removal of MB could be achieved in the photocatalytic process of rod-like g-C_3N_4 under visible light irradiation [23]. Although the g-C_3N_4 photocatalysis has been intensively explored in the past few years, most of which were focused on the degradation of dyes. However, as compared to dyes, the typical organic pollutants in water such as sulfonamides are colorless and more resistant to degradation.

Therefore, in the present work, four frequently-detected sulfonamides were selected, including sulfamethoxazole (SMX), sulfisoxazole (SSX), sulfadiazine (SDZ), sulfamerazine (SMZ). Their photocatalytic degradation behaviors by g-C_3N_4 under visible light irradiation were systematically investigated. The photocatalytic mechanism, including active species, oxidation products and degradation pathways for the four sulfonamides were also discussed and compared.

2. Materials and methods

2.1. Materials

Urea (analytically grade) was purchased from Sinopharm Chemical Reagent Co. Ltd., China. SMX (99% purity), SSX (99% purity), SDZ (99% purity), SMZ (99% purity) and humic acid were purchased from Sigma-Aldrich. Humic acid was used as a model natural organic matter (NOM) and purified according to the process described in the previous literature [24]. Briefly, 50 mg of humic acid was dissolved in 100 mL 0.1 M NaOH, stirred for 24 h and filtered through a 0.45 μm membrane. Then the filtrate was maintained at 4 °C. All other reagents were of analytical grade and used without further purification. All the solutions were prepared using deionized water.

2.2. Preparation of g-C_3N_4

The graphitic carbon nitride (g-C_3N_4) was prepared according to a method described in a previous study [25]. Briefly, 10 g of urea (AR, Sinopharm Chemical Reagent) was put into an alumina crucible with a cover and calcined at 550 °C for 3 h with a heating rate of 0.5 °C min^{-1} in a muffle furnace. After the thermal treatment, the obtained yellow colored powder was cooled to the room temperature naturally, washed thoroughly with distilled water and ethanol and then dried at 50 °C for 12 h.

2.3. Characterization of the synthesized g-C_3N_4

X-ray diffraction (XRD) patterns of the g-C_3N_4 samples were collected by a X-ray diffractometer (Philips, X Pert PRO MPD) utilizing Cu Kα radiation, and the accelerating voltage and applied current was set at 35 kV and 45 mA (λ = 0.15418 nm). The UV–vis diffuse reflectance spectra (UV-vis DRS) of g-C_3N_4 were achieved by a spectrophotometer (Shimadzu, UV2550).

2.4. Experimental procedures

2.4.1. Photodegradation of sulfonamides

A 300 W xenon lamp (Beijing NBeT) equipped with a 400 nm cut-off filter was used as the visible light source and the distance between reaction liquid interface and the light was 8 cm. In a typical process, 5 mg of g-C_3N_4 was uniformly suspended in 100 mL antibiotics aqueous solution (C_0 = 10 μM), and then stirred for 20 min to reach an adsorption/desorption equilibrium in the dark. After that, the solution was exposed to the visible light irradiation. And at given time intervals, 1.5 mL of the suspension was taken out, filtered through a 0.22 μm membrane and then analyzed by a high performance liquid chromatography (HPLC). During the reaction process, the temperature was maintained at 25 ± 2 °C. In addition, the initial pH of the antibiotics aqueous solution was adjusted to a pre-determined value by 0.01 M H_2SO_4 and 0.01 M NaOH.

2.4.2. Blank experiments

Photolysis of the sulfonamides without addition of the g-C_3N_4 was also conducted as the blank experiments under similar experimental conditions as described above.

2.4.3. ESR measurements

ESR spectra were employed to investigate the production of •OH and $^{\bullet}O_2^-$ by g-C_3N_4 under visible light irradiation. In the ESR detection experiments for hydroxyl radicals (DMPO–•OH), 10 mg g-C_3N_4 and 50 μL DMPO were mixed in 0.5 mL deionized water and stirred for 10 min, and then sampled by a 100 μL capillary tube, which was immediately inserted into the ESR cavity (Bruker A200 spectrometer). As for the detection of $^{\bullet}O_2^-$, 10 mg g-C_3N_4 and 50 μL DMPO were mixed in 0.5 mL CH_3OH and stirred for 10 min.

2.4.4. Trapping experiments of radicals and holes

The trapping experiments were carried out under the similar experimental conditions as that for photodegradation of sulfonamides, except that the specific scavengers were added into the suspension before visible light irradiation. The main oxidative species detected by the trapping experiments were $^{\bullet}O_2^-$, OH•, and

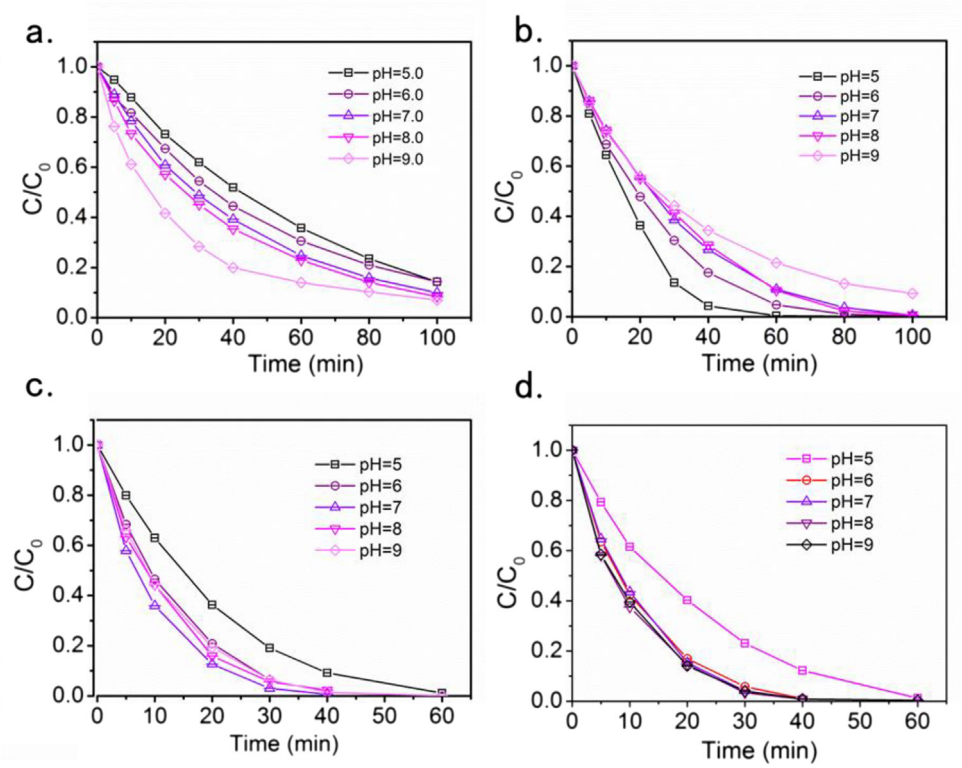

Fig. 2. Effect of initial pH on (a) SMX, (b) SSX, (c) SDZ and (d) SMZ photodegradation by g-C_3N_4 under visible irradiation.

Table 1
The kinetic constants (k) of the four sulfonamides.

Experiments	k(min^{-1})	R^2	Experiments	k(min^{-1})	R^2
SMX-Blank	2.04 E-4	0.977	SSX-Blank	2.48 E-4	0.973
SMX-g-C_3N_4	0.023	0.999	SSX-g-C_3N_4	0.041	0.987
SDZ-Blank	2.72 E-4	0.971	SMZ-Blank	2.88 E-4	0.924
SDZ-g-C_3N_4	0.125	0.971	SMZ-g-C_3N_4	0.078	0.995

holes by using EDTA-2Na (holes scavenger), *t*-BuOH (OH• scavenger) and purging N_2 ($^{\bullet}O_2^-$ scavenger), respectively [26].

2.5. Analytical methods

2.5.1. HPLC

SMX, SSX, SDZ and SMZ were analyzed by a HPLC (Waters e2695) with a UV–vis detector (waters 2489). The chromatographic separation was performed using a Waters symmetry C18 column (150 mm × 4.6 mm, 5 μm). The isocratic mobile phase consisted of 0.1% acetic acid and acetonitrile with the ratio of 70:30 (v/v). The flow rate of the mobile phase was set at 1 mL min^{-1}. The column temperature was maintained at 30 °C and the detection wavelength were 265 nm. The retention time for SMX, SSX, SDZ and SMZ were 4.64 min, 5.20 min, 2.47 min and 2.76 min, respectively.

2.5.2. Oxidation products

Ultra-performance liquid chromatography/MS/MS (Acquity UPLC, XEVO TQ MS) was used for the identification of transformation products generated during the photodegradation process. The UPLC column was Waters C18 column (Acquity UPLC BEH C18, 1.7 μm, 2.1×50 mm). To better detect the oxidation products, both isocratic elution and gradient elution were employed for the chromatographic separation in the UPLC/MS/MS analysis. The isocratic mobile phase was prepared by using 0.1% acetic acid and acetonitrile with the ratio of 70:30 (v/v), which was set at a flow rate of 0.1 mL min^{-1}. The gradient mobile phase was the combination of acetonitrile and 0.1% acetic acid. The gradient elution was programmed as follows: 0–1 min, 10% acetonitrile; 1–12 min, 10–90% acetonitrile; 12–15 min, 90% acetonitrile; 15–20 min, 10–90% acetonitrile. The flow rate was set at 0.1 mL^{-1} min. The MS data was obtained by a full scan mass from m/z 50 to 600 under positive ion mode. The cone voltage and capillary temperature were 30 kV and 600 °C, respectively. The MS/MS analysis was conducted under the same detection parameters as that of the MS analysis.

3. Results and discussion

3.1. Characterization of the synthesized g-C_3N_4

Fig. 1a shows the X-ray diffraction (XRD) pattern of the prepared g-C_3N_4. Two pronounced peaks can be seen at 13.1° and 27.4°. The peak of 13.1° relates to the in-plane structural packing motif of tri-*s*-triazine units, such as the hole-to-hole distance of the nitride pores in the crystal. While the peak of 27.4° corresponds to the interlayer stacking peak of aromatic systems [25]. The optical property of the synthesized g-C_3N_4 was exhibited by UV–vis diffuse reflectance, as shown in Fig. 1b. The band gap energy of the synthesized g-C_3N_4 can be determined by using the following formula [27]:

$$\alpha h\nu = A(h\nu\text{-}E_g)^{1/2}, \quad (1)$$

where α is the absorption coefficient, h is Planck constant, ν is the light frequency, A is the proportionality, and Eg is the band gap energy. The band gap of the synthesized g-C_3N_4 is calculated as 2.72 eV based on the data obtained from the UV–vis spectrum, which is close to the theoretical value (~2.70 eV).

3.2. Role of g-C_3N_4 in the photodegradation process

Experiments were conducted at an initial pH of 7.0 to investigate the role of g-C_3N_4 in photodegradation of the four sulfonamides under visible light irradiation. Fig. S1 compares the photodegrada-

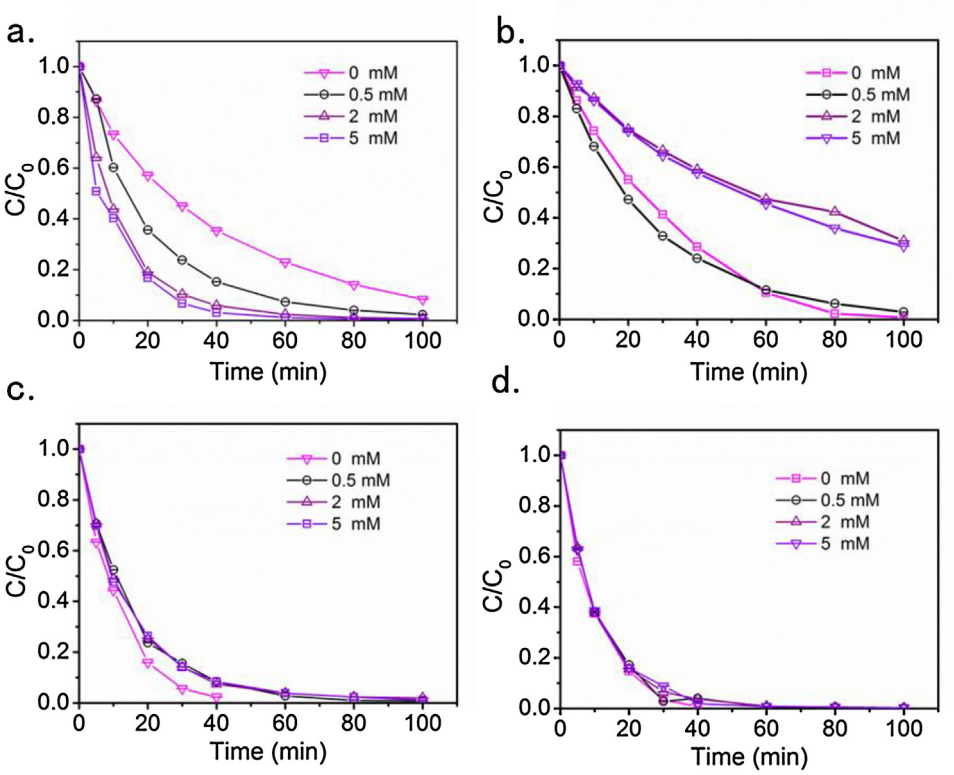

Fig. 3. Effect of HCO_3^- on (a) SMX, (b) SSX, (c) SDZ and (d) SMZ photodegradation by g-C_3N_4 under visible irradiation (initial pH = 8).

tion rates of the sulfonamides by photolysis (blank experiment) and that by g-C_3N_4 photocatalytic degradation. It can be seen that only <5% of the sulfonamides can be degraded within 100 min under visible light irradiation without g-C_3N_4. While in the presence of g-C_3N_4, the photodegradation efficiency increased substantially to above 95% for all the four sulfonamides, which indicated that the g-C_3N_4 possesses excellent visible-light photocatalytic activity for the degradation of them. Kinetic analysis showed that the photodegradation of the four sulfonamides followed first-order kinetics and the kinetic constants (k) were shown as Fig. S2 and Table 1. It could be seen that compared to photolysis, the kinetic constants for photocatalytic degradation of the four sulfonamides were dramatically increased with the addition of g-C_3N_4 under visible light irradiation. Besides, the stability of the synthesized g-C_3N_4 was also evaluated and a series of cyclic photocatalytic experiments were performed. After three cycles, the photocatalyst did not exhibit obvious loss of activity, as shown in Fig. S3. It exhibited that the synthesized g-C_3N_4 has the advantage of good stability.

3.3. Effect of water quality parameters on the photodegradation process

3.3.1. pH

As shown in Eq. (2), the $^{\bullet}O_2^-$ could be produced through the reaction of dissolved O_2 with a first photo induced electron, and H^+ in the water matrices could react with the produced $^{\bullet}O_2^-$ in the presence of a second photogenerated electron to produce H_2O_2 (Eq. (3)), which can finally turn into $^{\bullet}OH$ via Eq. (4) [28].

$$O_2 + e^- \rightarrow {}^{\bullet}O_2^- \quad (2)$$

$$^{\bullet}O_2^- + 2H^+ + e^- \rightarrow H_2O_2 \quad (3)$$

$$H_2O_2 + e^- \rightarrow {}^{\bullet}OH + OH^- \quad (4)$$

$$h^+ + OH^- \rightarrow {}^{\bullet}OH \quad (5)$$

Clearly, the H^+ concentration in the water (i.e. pH) can influence the generation and distribution of the oxidative species in the photodegradation process. Therefore, the effect of initial pH (i.e. pH = 5.0, 6.0, 7.0, 8.0, 9.0) on the degradation of sulfonamides by g-C_3N_4 under visible irradiation are investigated, as shown in Fig. 2. It can be seen that with the increase of initial pH, the degradation rates of SMX, SDZ and SMZ in the photodegradation process increased. When the pH value increased, H^+ concentration in solution decreased correspondingly, thus leading to the less consumption of $^{\bullet}O_2^-$ produced in the solution (Eq. (3)), which was shown to be the main reactive species for the photodegradation of SMX, SDZ and SMZ (see Section 3.3). On the contrary, for SSX, a decrease in the photodegradation efficiency was observed at higher pH. With the increase of pH value, the oxidizing ability of the photo-induced holes would be decreased possibly due to its electropositivity [29,30], thus leading to the decreased photodegradation efficiency. It should be noted that an increased pH was beneficial to the production of more $^{\bullet}OH$ via Eq. (5). However, the holes have been demonstrated to play a more important role in the photodegradation of SSX than $^{\bullet}OH$ (see Section 3.3). As an overall result, the photodegradation efficiency of SSX was reduced with the increase of solution pH.

3.3.2. HCO_3^-

Bicarbonate, as an inorganic compound, is ubiquitous in water, which is an important scavenger of $^{\bullet}OH$ as illustrated in Eqs. (6) and (7) [31]. To evaluate the influence of bicarbonate on the degradation of sulfonamides in the photodegradation process, experiments were conducted at different bicarbonate concentrations.

$$HCO_3^- + {}^{\bullet}OH \rightarrow {}^{\bullet}CO_3^- + H_2O,\ k = 8.5 \times 106\ M^{-1}\ s^{-1} \quad (6)$$

$$CO_3^{2-} + {}^{\bullet}OH \rightarrow {}^{\bullet}CO_3^- + HO^-,\ k = 3.9 \times 108\ M^{-1}\ s^{-1} \quad (7)$$

Typically, the conversion of $^{\bullet}OH$ to selective $^{\bullet}CO_3^-$ would reduce the degradation efficiency due to the lower reactivity of $^{\bullet}CO_3^-$ [32].

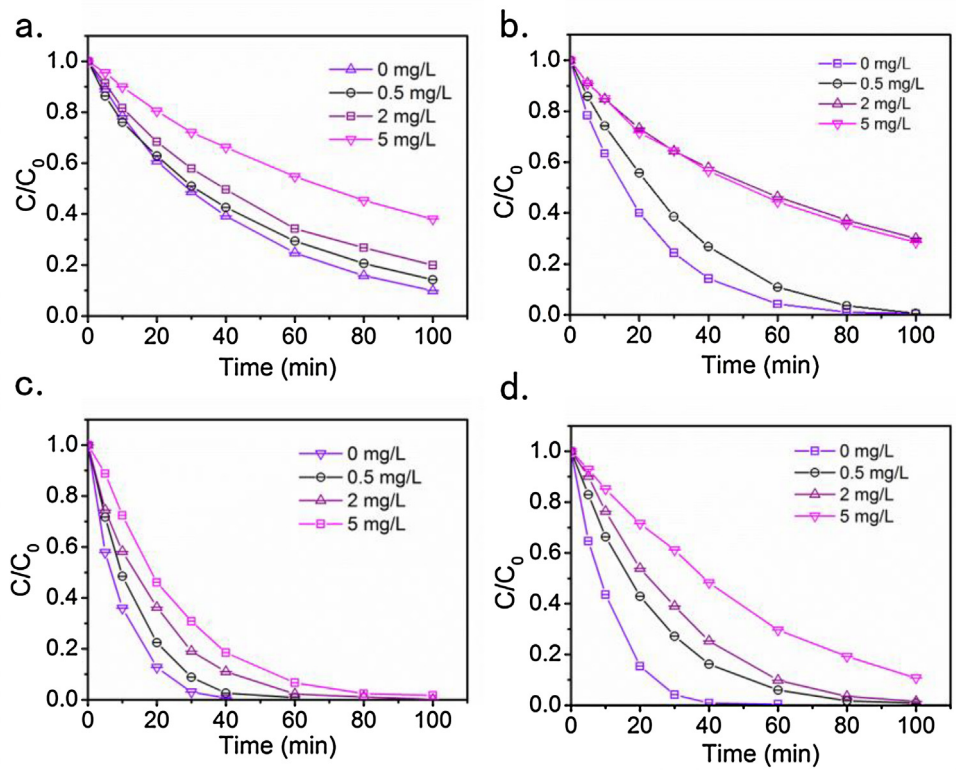

Fig. 4. Effect of HA on (a) SMX, (b) SSX, (c) SDZ and (d) SMZ photodegradation by g-C_3N_4 under visible irradiation (initial pH = 7).

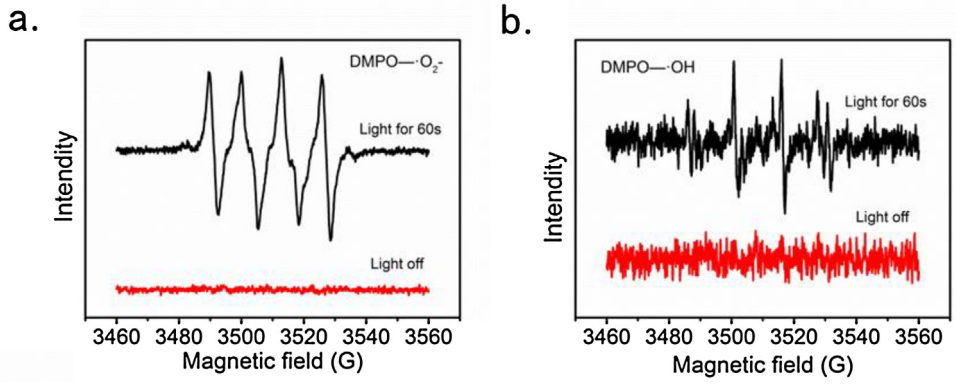

Fig. 5. ESR signals of the DMPO–$^{\bullet}O_2^-$ and DMPO–$^{\bullet}$OH.

However, as shown in Fig. 3a, the degradation efficiency of SMX was enhanced with the addition of HCO_3^- (varying from 0 to 5 mM). This might be attributed to the fact that $^{\bullet}$OH was not the main reactive species in the photodegradation process by g-C_3N_4 under visible irradiation, as discussed in detail in Section 3.3. And meanwhile, it was noticed that the solution pH exhibited a significant increase during the reaction process due to the addition of HCO_3^- (the final pH reached to ~8.5 from an initial value of 8.0), which can remarkably facilitate the photocatalytic degradation of SMX by g-C_3N_4 (as shown in Fig. 2a). On the contrary, an obvious inhibition effect of HCO_3^- was observed on the photocatalytic degradation of SSX, in which the oxidation was mainly performed by the $^{\bullet}$OH, as discussed in detail in Section 3.3. As for SDZ and SMZ, the addition of HCO_3^- exhibited negligible influence on the photodegradation efficiencies by g-C_3N_4. The reason might be that on one hand, $^{\bullet}$OH was not the main reactive species; and on the other hand, variation of solution pH from 8.0 to 8.5 had little effect on the photodegradation of these two sulfonamides (Fig. 2c and d).

3.3.3. HA

Humic acid, as an important constituent of natural organic matter, is present in both surface water and WWTP secondary effluents. Thus, the effect of HA on the photocatalytic degradation of the sulfonamides by g-C_3N_4 was investigated. As shown in Fig. 4, the photodegradation efficiencies of SMX and SSX was inhibited by the presence of HA. As the HA concentration increased from 0 to 5 mg L^{-1}, the photodegradation efficiencies of SMX and SSX decreased by 28.07 and 27.91%, respectively. As for SMZ and SDZ, the photodegradation rates in the process were also shown to be decreased even though the final removal was not influenced after 100 min of reaction. The inhibitory effect of HA on the photodegradation process can be explained by the two reasons below. Firstly, HA could compete with the sulfonamides for the active species produced in the solution [32]. Secondly, HA competes for photons with the g-C_3N_4, resulting in the less production of reactive species in the solution [33,34]. Nevertheless, the photodegradation efficiencies of the SMX, SSX, SDZ and SMX could still reach to 61.98, 71.56, 98.26

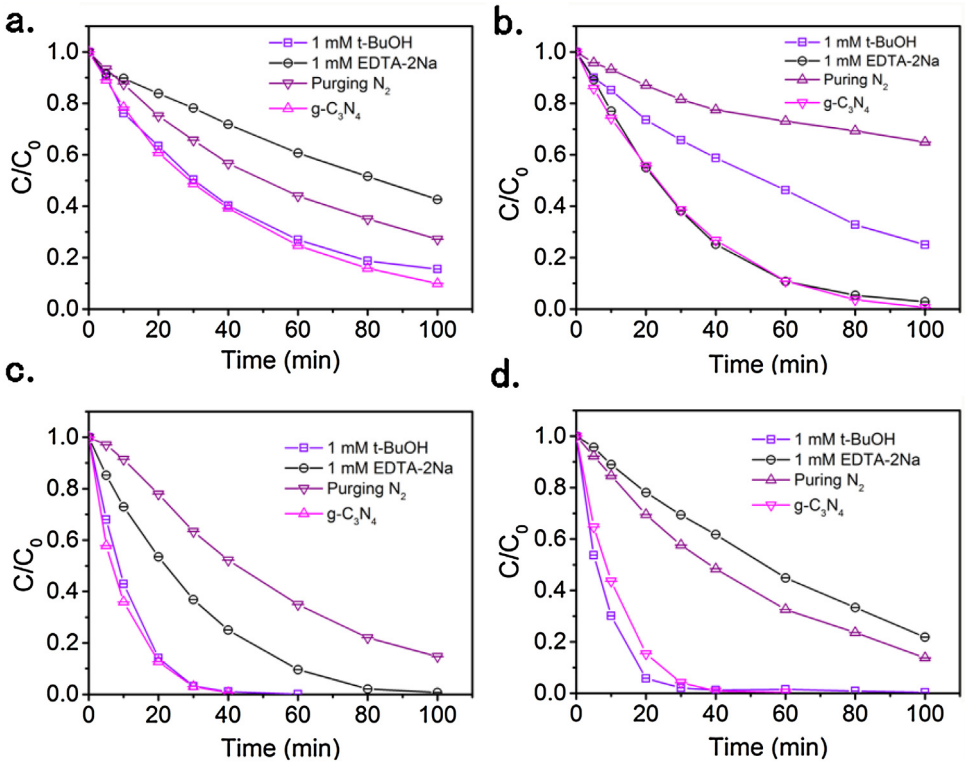

Fig. 6. Effects of a series of scavengers on the degradation efficiency of (a) SMX, (b) SSX, (c) SDZ and (d) SMZ by g-C_3N_4 under visible irradiation (initial pH = 7).

and 89.24%, respectively, even when the HA concentration was as high as 5 mg L^{-1}, demonstrating the robustness and effectiveness of the g-C_3N_4 photocatalytic process. In contrast, a dramatic reduction in the removal efficiency (~90%) has been reported for ozonation of SMX when 5 mg L^{-1} HA was present in the reaction solution [3].

3.4. Photocatalytic mechanism

3.4.1. Active species produced in photodegradation processes

In order to demonstrate photodegradation mechanism of the sulfonamides by g-C_3N_4 under visible light irradiation, ESR measurements and trapping experiments were conducted. As shown in Fig. 5, no ESR signals of DMPO-•O_2^- adduct and the DMPO-OH• adduct were observed in the dark. After visible light irradiation for 60s, the special spectrum with an intensity ration of 1:1:1:1 quartet signal was obvious observed, which was characteristic of the DMPO-•O_2^- adduct [35]. Moreover, a four-line ESR signal with intensity ration of 1:2:2:1 was also obtained, which corresponded to the assignment of the DMPO-•OH adduct [36]. This indicated that •O_2^- and OH• were produced in the photodegradation process by g-C_3N_4 under visible light irradiation. The role of •OH, •O_2^- and holes for the photodegradation of the sulfonamides was further identified by trapping experiments.

As shown in Fig. 6a, c and d, the photodegradation rate of SMX, SDZ and SMZ exhibited no obvious decrease in the presence of *t*-BuOH, indicating that •OH was not the dominant active species in the photocatalytic reaction. On the contrary, the photodegradation efficiencies of the three sulfonamides were significantly prevented by the addition of EDTA-2Na and purging N_2 respectively, implying that •O_2^- and holes were the main active species for photodegradation of the three sulfonamides by g-C_3N_4 under visible light irradiation. From Fig. 6b, the dramatic decrease of SSX photodegradation efficiency were both observed when addition of *t*-BuOH or purging N_2 were performed. However, addition of EDTA-2Na exhibited negligible influence on the SSX photodegradation process. The result suggested that holes and •OH were the main active species for SSX degradation by g-C_3N_4 under visible light irradiation.

3.4.2. Identification of oxidation products

To fully understand the photodegradation process of the sulfonamides by g-C_3N_4 under visible irradiation, UPLC/MS/MS analyses were further performed to identify the oxidation products of the four sulfonamides. The molecular structures and MS/MS fragmentation information of the oxidation products were summarized in Table 2.

For the photodegradation of SMX, a total of four oxidation products (A1–A4) were detected (Table 2), the corresponding MS spectra were shown in Figs. S4–S7. A1 (*m*/*z* 99 $[M+H]^+$) was identified as 3-amino-5-methylisoxazole, which was formed due to the cleavage of S-N bond on SMX (Fig. S4) [37]. A2 (*m*/*z* 270 $[M+H]^+$) was corresponding to the addition of 16 uma to the SMX (*m*/*z* 254 $[M+H]^+$), which could be attributed to the hydroxylation of SMX in the presence of •OH produced by g-C_3N_4 under visible irradiation. Furthermore, the MS^2 spectrum of A2 could be detected at *m*/*z* = 80, 99, 108, 124, 162 and 172 (Fig. S5), confirming the hydroxylation occurred on the benzene ring but not on isoxazole ring [3]. The MS^2 fragment ions of A3 (*m*/*z* 284 $[M+H]^+$) were detected at *m*/*z* = 122, 143, 182 and 189 (Fig. S6), indicating A3 (*m*/*z* 284 $[M+H]^+$) was formed by nitration of amino on the benzene ring [38]. Apart from these three common products mentioned above, A4 (*m*/*z* 503 $[M+H]^+$, *m*/*z* 525 $[M+Na]^+$), a dimeric product, was also observed in the photodegradation of SMX by g-C_3N_4 under visible irradiation. As shown in Fig. S7, the A4 could be identified as azo sulfamethoxazole according to its MS/MS spectrum. This intermediate product has been scarcely detected in previous studies with oxidation methods such as photolysis, ozonation, permanganate, photo-Fenton, and heterogeneous photocatalysis [3,37–40].

For the SSX photodegradation, three main products (B1, B2 and B3) were detected. B1 (*m*/*z* 110 $[M+H]^+$) was identifed as *p*-aminophenol according to its MS/MS spectrum (Fig. S8), which was

Table 2
The structure of products and their MS/MS fragments.

Molecular structure	Formula	UPLC/MS ([M+H])$^+$	UPLC/MS/MS (m/z)$^+$	Products
SMX				
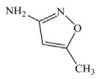	$C_4H_6N_2O$	99[a]	53, 79	A1
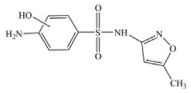	$C_{10}H_{11}N_3O_4S$	270[a]	80, 99, 108, 124, 158, 162, 172	A2
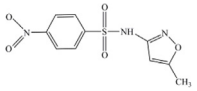	$C_{10}H_9N_3O_5S$	284[b]	122, 143, 182, 189	A3
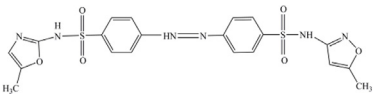		503[b]	160,174, 250,321	A4
SSX				
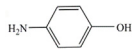	C_6H_7NO	110[a]	69, 82	B1
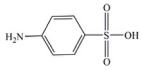	$C_6H_7NO_3S$	174[a]	65, 93, 94,115	B2
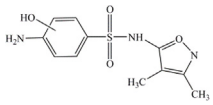	$C_{11}H_{13}N_3O_4S$	284[b]	69, 156, 173	B3
SDZ				
	$C_4N_3H_5$	96[b]	53, 79	C1
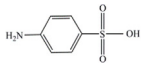	$C_6H_8N_2O_2S$	174[b]	57, 86, 105	C2
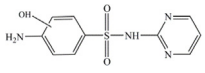	$C_{10}H_{10}N_4O_2S$	267[b]	69, 127, 156, 173	C3
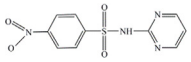	$C_{10}H_8N_4O_4S$	281[b]	75, 95, 122, 169, 265	C4
SMZ				
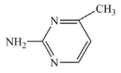	$C_5H_7N_3$	110[b]	66,69	D1
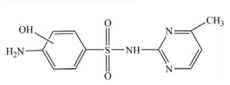	$C_{11}H_{12}N_4O_3S$	281[b]	87, 101, 131, 175	D2
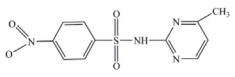	$C_{11}H_{10}N_4O_4S$	295[b]	92, 109, 122, 231, 249, 295	D3
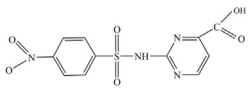	$C_{11}H_8N_4O_6S$	325[b]	87,101,112,130,175, 245	D4

[a] The products were detected by isocratic elution in the UPLC/MS/MS analysis.
[b] The products were detected by gradient elution in the UPLC/MS/MS analysis.

resulted from the bond-breaking between benzene ring and S bond. The MS/MS spectrum of B2 (m/z 174 [M+H]$^+$) was detected at 55, 65, 93, 94 and 115 (Fig. S9), which could be identified as sulfanilamide and formed through the bond-breaking of S-N. Similar to A2, the B3 (m/z 284 [M+H]$^+$) could be identified as the hydroxylated SSX formed by addition of •OH on benzene ring (Fig. S10).

For the SDZ, 4 photodegradation products, i.e. C1 (m/z 96 [M+H]$^+$), C2 (m/z 174 [M+H]$^+$), C3 (m/z 267 [M+H]$^+$) and C4 (m/z 281 [M+H]$^+$) were detected, as shown in Table 2. The C1 and C2 were identified as 2-aminopyrimidine and *p*-aminobenzene sulfonic acid, respectively. Via the cleavage of S-N bond, the SDZ was split into two parts, and thus the C1 and C2 were formed (Figs. S11 and S12), which has been separately reported by Feng [41] and Fabianska [5]. Similar to A2 and B3, C3 was the hydroxylation product of SDZ on its benzene ring (Fig. S13). The formation of C4 (m/z 281 [M+H]$^+$) could be attributed to the oxidation of the amidogen, yield-

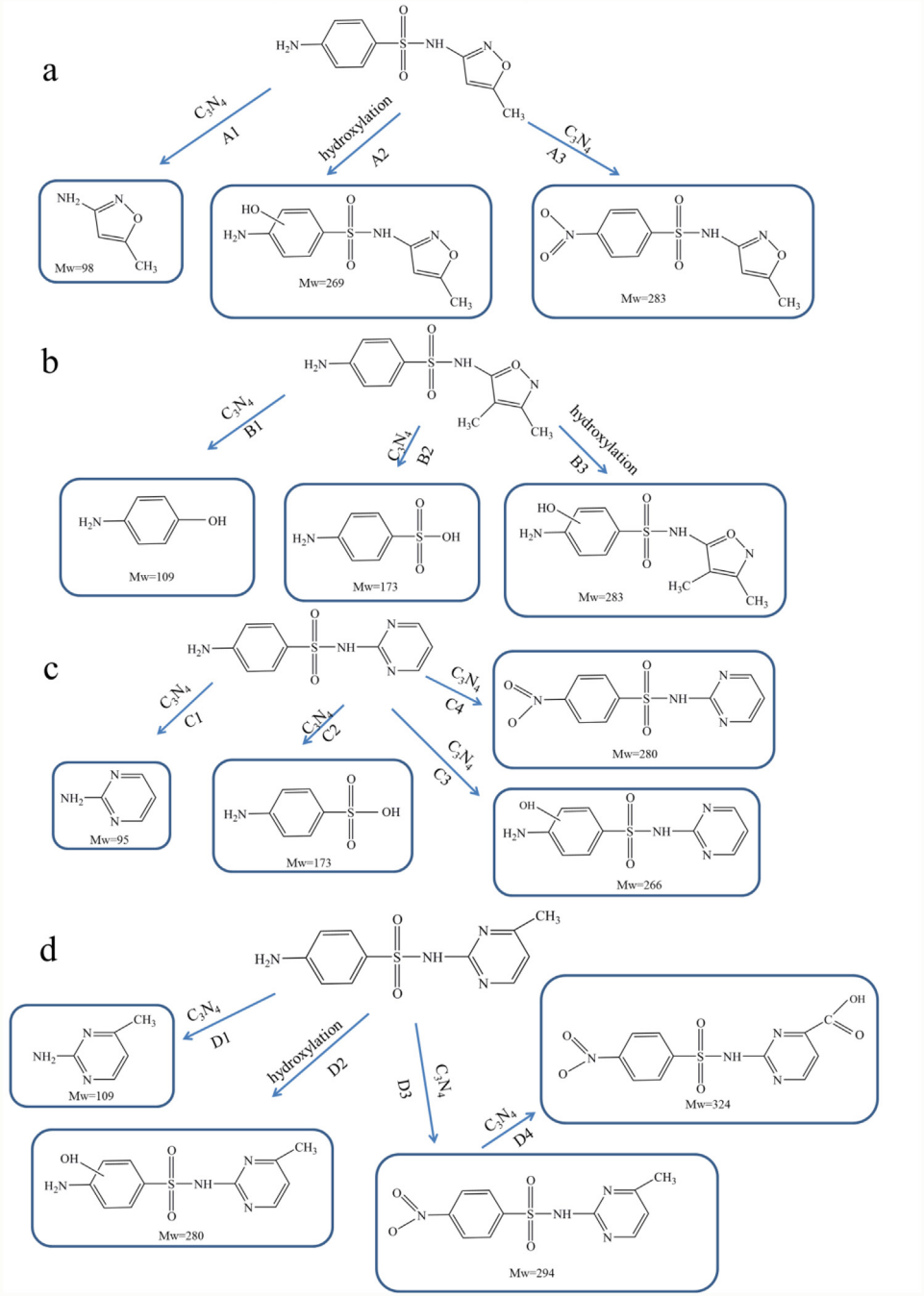

Fig. 7. Proposed pathways for reaction of (a) SMX, (b) SSX, (c) SDZ and (d) SMZ by g-C_3N_4 under visible light.

ing a nitro group on the benzene ring of SDZ (Fig. S14), as similar to the A3 in the photodegradation of SMX.

As for SMZ, four main products were detected. As shown in Fig. S15, the formation of D1 (m/z 110 $[M+H]^+$) could be attributed to the cleavage of S-N bond on SMZ. D2 (m/z 281 $[M+H]^+$) was identified as hydroxylated SMZ in the presence of OH• (Fig. S16). D3 (m/z 295 $[M+H]^+$) was considered as nitro-SMZ formed through the oxidation of amidogen on the benzene ring (Fig. S17). By further oxidation, the D3 (m/z 295 $[M+H]^+$) could be transformed to D4 (m/z 325 $[M+H]^+$) (Fig. S18) via carboxylation of the methyl group on SMZ.

3.4.3. *Proposed degradation pathways and comparison*

Based on the identification of the oxidation products (Table 2), the possible photodegradation pathways of the four sulfonamides have been proposed, as illustrated in Fig. 7. As can be seen, in the photodegradation process by g-C_3N_4 under visible light irradiation, there are two common degradation reactions shared by different sulfonamides, i.e. (I) the cleavage of S-N bond (A1, B2, C1 and D1) and (II) hydroxylation of the benzene ring (A2, B3, C3 and D2), which have both reported in photodegradation process by other photocatalyst. According to the previous reports, the cleavage of S-N bond owed to the attack of hydroxyl radical on the sulfonamide bond [5,37], resulting in the formation of A1, B2, C1 and D1. The hydroxylation of the benzene ring resulted from the addition of hydroxyl radical on the aromatic ring [37]. Though •OH was not the main active species for the photodegradation of SMX, SDZ and SMZ, both the cleavage of S-N bond and hydroxylation of the benzene ring occurred in the presence of •OH in the photodegradation process of the three sulfonamides by g-C_3N_4 under visible light irradiation.

It can be proposed that the cleavage of S-N and hydroxylation of the benzene ring were not the main reaction pathways in the three sulfonamides photodegradation processes, but the main pathways for SSX photodegradation, owing to the dominated role of •OH on the photodegradation of SSX.

More importantly, different photodegradation behaviors have also been observed among the four sulfonamides. For example, the oxidation of amine group to yield nitro group at the benzene ring occurred in the photodegradation of SMX, SDZ and SMZ to produce A3, C4 and D3 which is rarely reported in other photodegradation processes in previous studies, but not of the SSX. However, the bond cleavage between benzene ring and S only occurred in the photodegradation process of SSX. As for SMX, SDZ and SMZ, $^{\bullet}O_2^-$ and holes were the dominant reactive species in the photodegradation processes; while for SSX, •OH and holes have been demonstrated to play the major role. And the different oxidative species may have led to the different degradation pathways among the different sulfonamides. It could be speculated that $^{\bullet}O_2^-$ is beneficial to the oxidation of amine group to yield nitro group in the structure of sulfonamides. And the oxidation of amine group may be the main photodegradation pathway in the photodegradation of SMX, SDZ and SMZ, depending on the effect of active species on the photocatalytic efficiencies (Fig. 6). Furthermore, the methyl group in the structure of SMZ can be further oxidized to yield carboxyl group, resulting to the formation of D4. From the oxidation products, it can be find that the oxidation of the methyl group to yield carboxyl group only occurred in the SMZ photodegradation process even though SMX and SSX also contain a methyl group on their isoxazole rings, implying that the methyl group on pyrimidine derivatives (the case for SMZ) was easier to be oxidized than that on the isoxazole derivatives in the g-C_3N_4 visible-photodegradation system, which was similar to a previous study by Fabiańska et al. [5].

4. Conclusion

In this work, an effective visible-light photodegradation method for removal of the sulfonamides (SMX, SSX, SDZ and SMZ) was demonstrated with g-C_3N_4 as the catalyst. The photocatalytic degradation behaviors were systematically investigated.

(1) It was found that for the different sulfonamides, the water quality parameters such as pH, HCO_3^- and HA exhibited different influence on the photocatalytic degradation rate.
(2) The main reactive species that responsible for photodegradation of SMX, SDZ and SMZ were identified as $^{\bullet}O_2^-$ and holes through ESR measurements and tripping experiments; while the degradation of SSX was primarily performed by holes and •OH.
(3) The photodegradation pathways of the four sulfonamides were also proposed according to the oxidation products. It was indicated that except for common pathways shared by different sulfonamides, such as cleavage of S-N bond and hydroxylation of the benzene ring (the main pathways in degradation of SSX), there were also the specific pathways: i.e. nitration on the benzene ring only occurred for SMX, SDZ and SMZ (the main pathway in degradation of SMX, SDZ and SMZ); while the bond cleavage between benzene ring and S occurred only in SSX, and the carboxylation of the methyl group occurred only in SMZ.

Acknowledgements

This work was supported by the National Natural Science Foundation of China (No. 51678187), Open Project of State Key Laboratory of Urban Water Resource and Environment, Harbin Institute of Technology (No. QA201524), the Heilongjiang Postdoctoral Special Fund (No. LBH-TZ0409), and the Postdoctoral Scientific Research Developmental Fund of Heilongjiang Province (No.LBH-Q14070).

Appendix A. Supplementary data

Supplementary data associated with this article can be found, in the online version, at http://dx.doi.org/10.1016/j.apcatb.2017.03.059.

References

[1] K.S. Kim, K.K. Sang, Y.S. Mok, Chem. Eng. J. 271 (2015) 31–42.
[2] D.Y. Kong, B. Liang, Y. Hui, H.Y. Cheng, J.C. Ma, A.J. Wang, N.Q. Ren, Water Res. 72 (2015) 281–292.
[3] S.S. Gao, Z.W. Zhao, Y.P. Xu, J.Y. Tian, H. Qi, W. Lin, F.Y. Cui, J. Hazard. Mater. 274 (2014) 258–269.
[4] T. Zhang, B. Li, Crit. Rev. Env. Sci. Technol. 41 (2011) 951–998.
[5] A. Fabiańska, A. Białk-Bielińska, P. Stepnowski, S. Stolte, E.M. Siedlecka, J. Hazard. Mater. 280 (2014) 579–587.
[6] L. Sun, L.G. Chen, X. Sun, X.B. Du, Y.S. Yue, D.Q. He, H.Y. Xu, Q.L. Zeng, H. Wang, L. Ding, Chemosphere 77 (2009) 1306–1312.
[7] N. Le-Minh, S.J. Khan, J.E. Drewes, R.M. Stuetz, Water Res. 44 (2010) 4295–4323.
[8] K. Kümmerer, Chemosphere 75 (2009) 417–434.
[9] O. González, C. Sans, S. Esplugas, J. Hazard. Mater. 146 (2007) 459–464.
[10] I. Michael, L. Rizzo, C.S. Mcardell, C.M. Manaia, C. Merlin, T. Schwartz, C. Dagot, D. Fatta-Kassinos, Water Res. 47 (2013) 957–995.
[11] N. Ratola, A. Cincinelli, A. Alves, A. Katsoyiannis, J. Hazard. Mater 239–240 (2012) 1–18.
[12] Q.W. Bu, B. Wang, J. Huang, S.B. Deng, G. Yu, J. Hazard. Mater. 262 (2013) 189–211.
[13] W.J. Sim, J.W. Lee, E.S. Lee, S.K. Shin, S.R. Hwang, J.E. Oh, Chemosphere 82 (2011) 179–186.
[14] L.P. Padhye, H. Yao, F.T. Kung'u, C.H. Huang, Water Res. 51 (2014) 266–276.
[15] I. Keisuke, J.N. Naeimeh, G.E. Mohamed, Ozone Sci. Eng. 28 (2006) 353–414.
[16] D. Nasuhoglu, V. Yargeau, D. Berk, J. Hazard. Mater. 186 (2011) 67–75.
[17] K.P.D. Amorim, L.L. Romualdo, L.S. Andrade, Sep. Purif. Technol. 120 (2013) 319–327.
[18] E.S. Elmolla, M. Chaudhuri, J. Hazard. Mater. 173 (2010) 445–449.
[19] G.Z. Liao, S. Chen, X. Quan, H.T. Yu, H.M. Zhao, J. Mater. Chem. 22 (2012) 2721–2726.
[20] Y.J. Wang, R. Shi, J. Lin, Y.F. Zhu, Energy Environ. Sci. 4 (2011) 2922–2929.
[21] H.X. Zhao, S. Chen, X. Quan, H.T. Zhao, Appl. Catal. B: Environ. 194 (2016) 134–140.
[22] S.C. Yan, Z.S. Li, Z.G. Zou, Langmuir 25 (2009) 10397–10401.
[23] F. Jing, T.T. Chen, S.N. Liu, Q.H. Zhou, Y.M. Ren, Y.Z. Lv, Z.J. Fan, J. Colloid Interfaces Sci. 479 (2016) 1–6.
[24] Y. Laor, P.F. Strom, W.J. Farmer, Water Res. 33 (1999) 1719–1729.
[25] J. Liu, Y. Liu, N.Y. Liu, Y.Z. Han, X. Zhang, H. Huang, Y. Lifshitz, S. Lee, J. Zhong, Z.H. Kang, Science 347 (2015) 970–974.
[26] Y.H. Lv, C.S. Pan, X.G. Ma, R.L. Zong, X.J. Bai, Y.F. Zhu, Appl. Catal.: B Environ. 138–139 (2013) 26–32.
[27] S. Ye, L.G. Qiu, Y.P. Yuan, Y.J. Zhu, J. Xia, J.F. Zhu, J. Mater. Chem. A 1 (2013) 3008–3015.
[28] Y.J. Cui, Z.X. Ding, P. Liu, M. Antonietti, X.Z. Fu, X.C. Wang, Phys. Chem. Chem. Phys. 14 (2012) 1455–1462.
[29] U.G. Akpan, B.H. Hameed, J. Hazard. Mater. 170 (2009) 520–529.
[30] W.D. Shi, Y. Yan, Y. Xu, Chem. Eng. J. 215–216 (2013) 740–746.
[31] J.X. Yang, J. Li, W.Y. Dong, J. Ma, J. Cao, T.T. Li, J.Y. Li, J. Gu, P.X. Liu, J. Hazard. Mater. 316 (2016) 110–121.
[32] Y. Yang, J. Jiang, X. Lu, J. Ma, Y.Z. Liu, Environ. Sci. Technol. 49 (2015) 7330–7339.
[33] Q. Zhao, L. Feng, X. Cheng, C. Chao, L.Q. Zhang, Water Sci. Technol. 67 (2013) 1605–1611.
[34] K.H. Chan, W. Chu, Water Res. 39 (2005) 2154–2166.
[35] H. Zhang, L.X. Zhao, F.L. Geng, L.H. Guo, B. Wan, Y. Yang, Appl. Catal.: B Environ. 180 (2016) 656–662.
[36] H. Wang, Y. Su, H.X. Zhao, H.T. Yu, S. Chen, Y.B. Zhang, Q. Xie, Environ. Sci. Technol. 48 (2014) 11984–11990.
[37] L.H. Hu, P.M. Flanders, P.L. Miller, T.J. Strathmann, Water Res. 41 (2007) 2612–2626.
[38] M.D.M. Gómez-Ramos, M. Mezcua, A. Agüera, A.R. Fernández-Alba, J. Hazard. Mater. 192 (2011) 18–25.
[39] A.G. Trovó, R.F.P. Nogueira, A. Agüera, A.R. Fernández-Alba, C. Sirtori, S. Malato, Water Res. 43 (2009) 3922–3931.
[40] A.G. Trovó, R.F.P. Nogueira, A. Agüera, C. Sirtori, A.R. Fernández-Alba, Chemosphere 277 (2009) 1292–1298.
[41] Y. Feng, D.L. Wu, D. Yu, T. Zhang, K. Shih, Environ. Sci. Technol. 50 (2016) 3119–3127.